

Beyond the neutron-drip line: two-neutron decay of unbound nuclei

K. HAGINO^{1,2} and H. SAGAWA^{3,4}

¹ *Department of Physics, Tohoku University, Sendai, 980-8578, Japan*

² *Research Center for Electron Photon Science, Tohoku University, 1-2-1 Mikamine, Sendai 982-0826, Japan*

³ *RIKEN Nishina Center, Wako 351-0198, Japan*

⁴ *Center for Mathematics and Physics, University of Aizu, Aizu-Wakamatsu, Fukushima 965-8560, Japan*

(Received)

We discuss a decay of unbound nuclei beyond the neutron drip-line using a three-body model with a core nucleus and two valence neutrons. We particularly discuss the role of dineutron correlation between the valence neutrons in the two-neutron emission from the ground state of ^{26}O and ^{10}He nuclei. Our calculations clearly indicate that the emission of the two neutrons in the back-to-back direction is enhanced due to the dineutron correlation.

KEYWORDS: neutron dripline, resonance, dineutron correlation, three-body model

1. Introduction

An important question in physics of unstable nuclei is: where are the neutron and the proton drip-lines located in the nuclear chart? On the neutron side, the drip-line has so far been identified experimentally up to oxygen isotopes [1], which is being extended in new measurements e.g., at RIBF in RIKEN. In this connection, an interesting phenomenon has been found in the neutron drip-line for oxygen isotopes. That is, while the drip-line nucleus for oxygen is ^{24}O (with the neutron number of $N=16$), the drip-line extends considerably for fluorine isotopes, for which at least up to ^{31}F (with $N=22$) is bound [1]. This phenomenon has been referred to as oxygen anomaly [2], for which Otsuka and his collaborators have successfully explained in terms of the three-body and the tensor interactions [2, 3].

Partly motivated by the oxygen anomaly, in this contribution we discuss the decay dynamics of the unbound ^{26}O nucleus, which is located beyond the neutron drip-line. The decay of ^{26}O has attracted lots of attention in recent years both experimentally [4–8] and theoretically [9–19]. We shall use here a three-body model with an inert ^{24}O core and two valence neutrons, and clarify the role of neutron-neutron correlation in the decay of ^{26}O [12–14]. We shall apply a similar model also to ^{10}He and discuss the angular correlation of the two emitted neutrons from a spontaneous decay of the unbound ^{10}He nucleus.

2. Two-neutron decay of ^{26}O

2.1 The decay energy spectrum

We first discuss the unbound ^{26}O nucleus. There have been three measurements for the decay energy spectrum of ^{26}O , at Michigan State University (MSU) [4], GSI [5], and RIKEN [8]. In all of these three measurements, a proton knockout reaction of ^{27}F has been used to produce ^{26}O , which then spontaneously decays to $^{24}\text{O} + n + n$. The decay energy of ^{26}O has been determined in the RIKEN

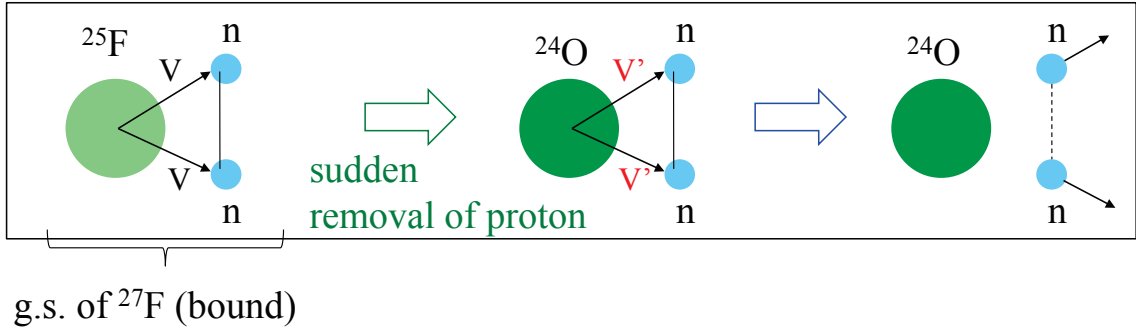


Fig. 1. A schematic illustration of the three-body model calculation for the two-neutron decay of ^{26}O .

measurement to be 18 ± 3 (stat) ± 4 (syst) keV [8]. The ^{26}O nucleus was therefore almost bound if the nuclear interaction was a little bit stronger. In reality, the interaction is not strong enough so that the ground state of ^{26}O appears as a resonance state.

To describe the two-neutron decay of ^{26}O , we employ a three-body model. The Hamiltonian in this model reads,

$$H = h_{nC}(1) + h_{nC}(2) + v(\mathbf{r}_1, \mathbf{r}_2), \quad (1)$$

where h_{nC} is a single-particle Hamiltonian for the relative motion between a neutron and the core nucleus, and $v(\mathbf{r}_1, \mathbf{r}_2)$ is the interaction between the valence neutrons. For simplicity, we have neglected the off-diagonal component of the recoil kinetic energy of the core nucleus [12–14]. For the interaction v , we take a contact interaction whose strength depends on the density [20–22], that is,

$$v(\mathbf{r}_1, \mathbf{r}_2) = \delta(\mathbf{r}_1 - \mathbf{r}_2) \left(v_0 + \frac{v_\rho}{1 + \exp[(r_1 - R_\rho)/a_\rho]} \right), \quad (2)$$

where the strength v_0 for the density independent part is determined from the scattering length for nn scattering [23], while the parameters for the density dependent part, v_ρ , R_ρ , and a_ρ , are adjusted to reproduce the ground state energy.

Figure 1 illustrates schematically how the three-body model can be applied to the two-neutron decay of ^{26}O nucleus [12, 14]. Since the ^{26}O nucleus is produced experimentally from ^{27}F , we first apply the three-body model to the ^{27}F nucleus and construct the bound ground state wave function of this nucleus as $\Psi_{nn}(^{27}\text{F}) \otimes |^{25}\text{F}\rangle$, where $\Psi_{nn}(^{27}\text{F})$ is the wave function for the two valence neutrons while $|^{25}\text{F}\rangle$ is the ground state wave function for the core nucleus, ^{25}F . We then assume a sudden removal of proton from the core nucleus. That is, the core nucleus suddenly changes from ^{25}F to ^{24}O while the two neutron configuration, $\Psi_{nn}(^{27}\text{F})$, remain the same, therefore the three-body wave function becomes $\Psi_{nn}(^{27}\text{F}) \otimes |^{24}\text{O}\rangle$. The sudden removal of proton also accompanies a change in the single-particle Hamiltonian, h_{nC} . Since the wave function $\Psi_{nn}(^{27}\text{F}) \otimes |^{24}\text{O}\rangle$ is not an eigenfunction of the three-body model Hamiltonian for ^{26}O , it forms a wave packet. Because ^{26}O does not have a bound state, the wave function then spontaneously evolves in time and the two valence neutrons fly away from the core nucleus, ^{24}O . The decay energy spectrum can be constructed by taking an overlap between the initial wave function, $\Psi_{nn}(^{27}\text{F})$, and the two-particle wave function for ^{26}O , $\Psi_{nn}(^{26}\text{O}; E)$, as

$$\frac{dP}{dE} = |\langle \Psi_{nn}(^{27}\text{F}) | \Psi_{nn}(^{26}\text{O}; E) \rangle|^2. \quad (3)$$

We mention that a very similar idea has been put forward also by Tsukiyama, Otsuka, and Fujimoto, who studied the decay of ^{25}O and ^{26}O using a shell model [15].

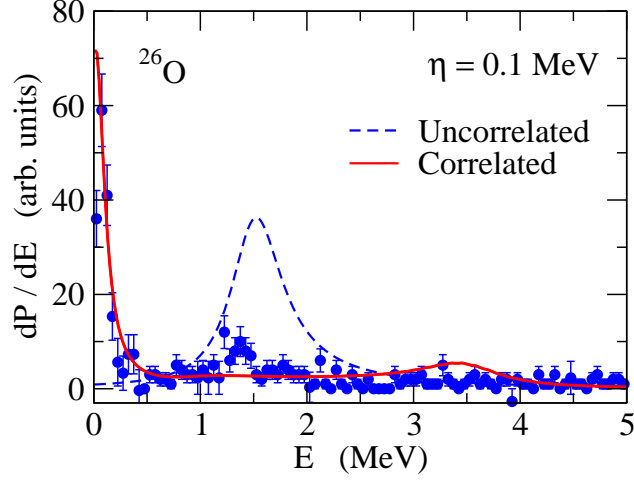


Fig. 2. The decay energy spectrum for ^{26}O obtained with the three-body model. The dashed line shows the result for the uncorrelated case, in which the nn interaction is set to zero. The solid line shows the result for the full correlated case. The experimental data are taken from Ref. [8].

The decay energy spectrum, Eq. (3), can be expressed also in terms of the Green's function as,

$$\frac{dP}{dE} = \int dE' |\langle \Psi_{E'} | \Phi_{\text{ref}} \rangle|^2 \delta(E - E') = \frac{1}{\pi} \Im \left\langle \Phi_{\text{ref}} \left| \frac{1}{H - E - i\eta} \right| \Phi_{\text{ref}} \right\rangle, \quad (4)$$

where $|\Phi_{\text{ref}}\rangle \equiv |\Psi_{nn}(^{27}\text{F})\rangle$ is the initial (reference) state, and \Im denotes the imaginary part. Notice that $1/(H - E - i\eta)$, is nothing but the Green's function, $G(E)$, with η being an infinitesimally small positive number. The Green's function can be constructed with the uncorrelated Green's function, $G_0(E) = 1/(h_{nC}(1) + h_{nC}(2) - E - i\eta)$, as [24],

$$G(E) = G_0(E) - G_0(E)v(1 + G_0(E)v)^{-1}G_0(E). \quad (5)$$

Since we employ a contact interaction for v , this equation can be solved most easily in the coordinate space [20, 24].

Figure 2 shows the decay energy spectrum of ^{26}O so obtained. To this end, we employ a simple uncorrelated $(1d_{3/2})^2$ configuration in ^{27}F for the initial reference state, $|\Phi_{\text{ref}}\rangle$. We also keep η to be a finite value, $\eta = 0.1$ MeV, for a presentation purpose. When the nn interaction is set to zero in the three-body Hamiltonian for ^{26}O , the initial reference state, $|\Phi_{\text{ref}}\rangle$, has a large overlap with the $(1d_{3/2})^2$ configuration in ^{26}O , for which the $1d_{3/2}$ resonance state in ^{25}O is located at 749 keV [8]. The decay energy spectrum then has a peak at twice this energy, 1.498 MeV (see the dashed line). When the nn interaction is switched on, the peak is shifted largely towards lower energies. If the parameters for the nn interaction are adjusted to the ground state energy of ^{26}O , the experimental decay energy spectrum is well reproduced with this calculations, as is indicated by the solid line in the figure.

2.2 The 2^+ state

The experimental data shown in Fig. 2 show a prominent secondary peak at $E = 1.28_{-0.08}^{+0.11}$ MeV [8]. This is most likely the 2^+ state in ^{26}O , while the dominant peak at 18 keV is due to the 0^+ state. Our three-body model calculation yields the 2^+ peak at 1.282 MeV with the width of $\Gamma = 0.12$ MeV [14], which agrees perfectly with the experimental data. An important fact here is that the energy shift from the uncorrelated case, 1.498 MeV, is much smaller for the 2^+ state as compared to the ground state 0^+ state. This is typically the case for a single- j configuration with a pairing interaction [25],

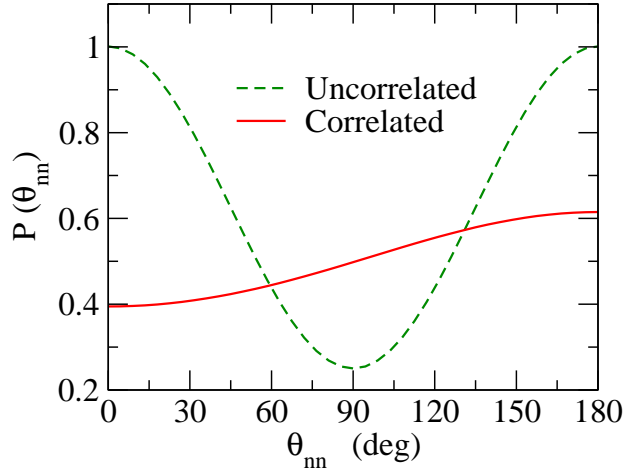


Fig. 3. The angular correlation in the momentum space for the two valence neutrons emitted from the decay of ^{26}O . The dashed and the solid curves show the results of the uncorrelated and the correlated cases, respectively.

in which the overlap between the wave functions for the two neutrons in 2^+ state is much smaller than that in 0^+ state, and thus the energy gain due to the pairing interaction is much smaller. Of course, the dineutron correlation, that is, a mixture of several configurations, also plays an important role, especially for the 0^+ state, but the relative position of the 0^+ and 2^+ peaks, with respect to the uncorrelated energy, can be qualitatively understood in this way. We mention that a similar result has been obtained recently also with a Gamow shell model calculation [17].

2.3 The angular correlation

Let us now discuss the angular correlation between the emitted two valence neutrons. Very roughly speaking, the angular correlation can be computed as,

$$P(\theta_{nn}) \sim 4\pi \int dk_1 dk_2 |\langle k_1 k_2, \theta_{nn} | \Psi_{nn}(E) \rangle|^2, \quad (6)$$

where $|k_1 k_2, \theta\rangle$ is an uncorrelated wave function for the valence neutrons with the asymptotic wave numbers of $\mathbf{k}_1 = (k_1, \hat{\mathbf{k}}_1 = 0)$ and $\mathbf{k}_2 = (k_2, \hat{\mathbf{k}}_2 = \theta_{nn})$. $|\Psi_{nn}(E)\rangle$ is a three-body wave function obtained with the three-body model at $E = (k_1^2 \hbar^2 + k_2^2 \hbar^2)/(2\mu)$, where μ is the reduced mass between a valence neutron and the core nucleus. See Refs. [12, 14, 24] for a more accurate formula with phase shifts and the Green's function.

Figure 3 shows the angular distribution for the decay of ^{26}O . The dashed and the solid lines show the results for the uncorrelated and the correlated cases, respectively. In the uncorrelated case, the angular correlation is symmetric with respect to $\theta_{nn} = \pi/2$. On the other hand, for the correlated case, the component for large angles is enhanced while the small angle component is significantly suppressed. The angular distribution then becomes asymmetric, with an enhancement of back-to-back emissions. This is as a natural consequence of the dineutron correlation [26], with which the valence neutrons are spatially localized at a similar position inside a nucleus. The localization in the coordinate space corresponds to a large relative momentum for the two neutrons [14], which can be understood from a view of uncertainty relation. Once the two neutrons are emitted outside the core nucleus, the two neutrons then move in the opposite direction. This clearly indicates that an observation of the enhancement of back-to-back emission makes a direct experimental evidence for the dineutron correlation. Another three-body model calculation by Grigorenko *et al.* has also yielded a similar enhancement of back-to-back emission [10].

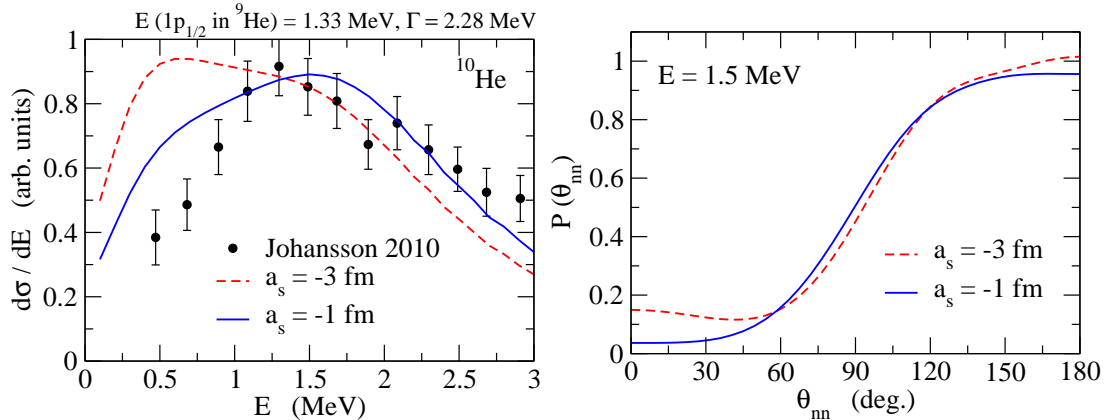


Fig. 4. (Left panel) The decay energy spectrum for the ^{10}He nucleus obtained with a three-body model of $^8\text{He}+n+n$. The dashed and the solid lines are obtained with the s -wave scattering length for the n - ^8He scattering of $a_s = -3$ fm and -1 fm, respectively. The experimental data are taken from Ref. [27]. (Right panel) The angular correlation for the emitted two neutrons from the two-neutron decay of ^{10}He at the decay energy of $E=1.5$ MeV. The meaning of each line is the same as in the left panel.

3. Two-neutron decay of ^{10}He

Let us next discuss the two-neutron decay of ^{10}He . In the experiments reported in Ref. [27], the ^{10}He nucleus was produced by a proton knockout reaction from ^{11}Li . The experimental decay energy spectrum shows a prominent peak at 1.54(11) MeV with a width of $\Gamma = 1.91$ (41) MeV [27], which has been confirmed recently with a $2p2n$ -removal reaction from ^{14}Be [28]. See also Ref. [29] for an earlier measurement.

On the other hand, the structure of ^9He nucleus, which is used to calibrate the parameters for the three-body model for ^{10}He , has been poorly understood. The authors of Ref. [27] fitted the observed decay energy spectrum with a narrow $1/2^-$ resonance at 1.33(8) MeV, whose width has been deduced to be $\Gamma=0.10(6)$ MeV using $^9\text{Be}(^{14}\text{C}, ^{14}\text{O})^9\text{He}$ reaction [30]. This resonance state has been identified at 2.0 ± 0.2 MeV with a width of ~ 2 MeV, and at 1.235 ± 0.115 MeV with a width of 130_{-130}^{+170} keV in Refs. [31] and [32], respectively. In contrast, a recent high-resolution measurement of $^8\text{He}+p$ scattering does not support a narrow $1/2^-$ resonance in ^9He [34]. In addition to the $1/2^-$ resonance, many experimental data also show a large strength close to the threshold, which is interpreted as an s -wave virtual state. The experimental data have been fitted with the s -wave scattering length for n - ^8He scattering of $a_s = -3.17(66)$ [27], $a_s > -20$ fm [31], $a_s = -12 \pm 3$ fm [32], and $a_s < -10$ fm [33], among which the value in Ref. [27] seems incompatible with the others. On the other hand, the measurement reported in Ref. [34] has suggested a broad $1/2^+$ state at approximately 3 MeV above the threshold, rather than near the threshold.

Even though there is a large uncertainty in the structure of the ^9He nucleus, we perform a three-body model calculation for the two-neutron decay of ^{10}He assuming a $^8\text{He}+n+n$ structure. To this end, we assume a simple $(1s_{1/2})^2(1p_{3/2})^4$ structure for the neutron configuration of the core nucleus, ^8He , even though an actual structure may be much more complex [35]. For the neutron-core potential, we introduce a parity-dependent Woods-Saxon potential. For negative parity states, we adjust the parameters to reproduce the $p_{1/2}$ resonance at 1.33 MeV. Such potential, however, yields a much larger resonance width, with an order of MeV, as compared to the width of around 0.1 MeV observed in Refs. [30, 32]. This may be due to either an artifact of our assumption of a simple structure for the ^8He nucleus or the experimental uncertainty of the $p_{1/2}$ resonance state, as the calculated width is consistent with the observed width reported in Ref. [31]. For even partial waves, we vary the depth

parameter of the Woods-Saxon potential in order to investigate the dependence of the results on the the s -wave scattering length, a_s . In the three-body model calculations, we include partial waves up to $\ell = 14$ with an energy cut-off of 30 MeV.

The dashed line in the left panel of Fig. 4 shows the decay energy spectrum of ^{10}He obtained with $a_s = -3$ fm, which is close to the empirical value of Ref. [27]. In this calculation, we use the ground state wave function for ^{11}Li obtained with a three-body model [21] as a reference state, Φ_{ref} , and also a similar density-dependent contact interaction as the one used in Ref. [21] for the interaction between the valence neutrons in ^{10}He . As one can see in the figure, this calculation does not reproduce well the observed decay energy spectrum. Again, this may be due to the simple structure assumed for the core nucleus, ^8He . By changing the value of s -wave scattering length from $a_s = -3$ fm to $a_s = -1$ fm, one could make the calculation agree better with the experimental data, as is indicated by the solid line in the figure, even though this value of scattering length is inconsistent with the experimental values.

The angular correlation for the emitted two neutrons is plotted in the right panel of Fig. 4 for the decay energy of $E=1.5$ MeV. As in the ^{26}O nucleus shown in Fig. 3, the back-to-back emission is considerably enhanced due to the dineutron correlation. It is interesting to notice that the angular correlation is less sensitive to the value of the s -wave scattering length as compared to the decay energy spectrum. Evidently, the angular correlation provides a good probe for the dineutron correlation, which has otherwise been difficult to observe experimentally.

4. Summary and future perspectives

We have discussed the two-neutron emission decay of unbound nuclei beyond the neutron drip-line using the three-body model with a density dependent contact interaction between the valence neutrons. We have first calculated the decay energy spectrum for ^{26}O using a method based on the two-particle Green's function, which is easy to evaluate in the coordinate space with a contact interaction. We have shown that a peak in the energy spectrum is considerably shifted towards low energies due to the interaction between the valence neutrons. By adjusting the parameters for the interaction so that the ground state energy is reproduced, we have shown that one can achieve an excellent agreement with the experimental data for the excited 2^+ state. We have then investigated the angular correlation of the two emitted neutrons, and have shown that an emission of the two neutrons in the opposite direction (that is, the back-to-back emission) is enhanced due to the dineutron correlation. We have applied the same model also to the ^{10}He nucleus assuming a simple $p_{3/2}$ -closed structure for the core nucleus, ^8He . As in ^{26}O , we have found that the back-to-back two-neutron emission is preferred in the decay of ^{10}He .

As we have discussed in this contribution, two-neutron decays of unbound nuclei provide an important probe for the dineutron correlation inside nuclei. The dineutron correlation has been predicted theoretically for some time, but it has not been straightforward to probe it experimentally. In the Coulomb dissociation of Borromean nuclei, one can use the cluster sum rule to deduce the mean value of the opening angle between the valence neutrons [36–38]. The extracted mean opening angles for ^{11}Li and ^6He are significantly smaller than the value for the uncorrelated case [36–38], that is, $\langle\theta_{nn}\rangle=90$ degrees, clearly indicating the existence of the dineutron correlation in these Borromean nuclei. A small problem in this analysis is, however, that one can access only to the mean value of a distribution and the detailed distribution cannot be probed.

The two-proton radioactivity, that is, a spontaneous emission of two valence protons, of proton-rich nuclei [39] has been expected to provide an alternative tool to probe the nucleon-nucleon correlation in the initial wave function. An attractive feature of this phenomenon is that the two valence protons are emitted directly from the ground state even without any external perturbation. The long range interaction between the two protons, however, make theoretical analyses quite complicated, and it may not be straightforward to probe the diproton correlation from this phenomenon.

The two-neutron decay of unbound nuclei beyond the neutron-drip line is an analogous process of the two-proton radioactivity, corresponding to a penetration of two neutrons over a centrifugal barrier. Since the long range Coulomb interaction is absent, the dineutron correlation may be better probed using the two-neutron decays. In this context, we have argued in this contribution that an enhancement of back-to-back emission makes a direct evidence for the dineutron correlation. Its observation has remained as an experimental challenge, especially for the ^{26}O nucleus, for which the decay energy is considerably small. Another experimental challenge is to measure the spin of the emitted two neutrons, which would carry an important information on the nn correlation inside a nucleus.

A theoretical challenge, on the other hand, is to extend the three-body model by including the core deformation. This will be important in discussing the two-neutron decay of the ^{16}Be nucleus [40]. Another important challenge is an extension from the three-body to multi-body descriptions. For the two-neutron decay of ^{13}Li [27, 41] and ^{10}He , the nuclei ^{11}Li and ^8He would not make a good core, and such extension will be important. That is, a five-body description for ^{13}Li with $^9\text{Li}+4n$ and a seven-body description for ^{10}He with $^4\text{He}+6n$ would provide better results. One will also be able to apply a five-body model to four-neutron emission decays, such as a decay of ^{28}O nucleus. A measurement for the decay of ^{28}O has already been carried out in RIKEN and the experimental data have now been under analysis [42]. It will therefore be a very important future direction to develop a theoretical model based on a five-body model which is applicable to the four-neutron emission decay of ^{28}O .

Acknowledgments

We thank T. Nakamura and Y. Kondo for useful discussions. This work was supported by JSPS KAKENHI Grant Number 16H02179.

References

- [1] H. Sakurai *et al.*, Phys. Lett. **B448**, 180 (1999).
- [2] T. Otsuka, T. Suzuki, J.D. Holt, A. Schwenk, and Y. Akaishi, Phys. Rev. Lett. **105**, 032501 (2010).
- [3] T. Otsuka, T. Suzuki, R. Fujimoto, H. Grawe, and Y. Akaishi, Phys. Rev. Lett. **95**, 232502 (2005).
- [4] E. Lunderberg *et al.*, Phys. Rev. Lett. **108**, 142503 (2012).
- [5] C. Caesar *et al.*, Phys. Rev. **C88**, 034313 (2013).
- [6] Z. Kohley *et al.*, Phys. Rev. Lett. **110**, 152501 (2013).
- [7] Z. Kohley *et al.*, Phys. Rev. **C91**, 034323 (2015).
- [8] Y. Kondo *et al.*, Phys. Rev. Lett. **116**, 102503 (2016).
- [9] L.V. Grigorenko, I.G. Mukha, C. Scheidenberger, and M.V. Zhukov, Phys. Rev. **C84**, 021303(R) (2011).
- [10] L.V. Grigorenko, I.G. Mukha, and M.V. Zhukov, Phys. Rev. Lett. **111**, 042501 (2013).
- [11] L.V. Grigorenko and M.V. Zhukov, Phys. Rev. **C91**, 064617 (2015).
- [12] K. Hagino and H. Sagawa, Phys. Rev. **C89**, 014331 (2014).
- [13] K. Hagino and H. Sagawa, Phys. Rev. **C90**, 027303 (2014).
- [14] K. Hagino and H. Sagawa, Phys. Rev. **C93**, 034330 (2016).
- [15] K. Tsukiyama, T. Otsuka, and R. Fujimoto, Prog. Theor. Exp. Phys. **2015**, 093D01 (2015).
- [16] K. Fosse, J. Rotureau, N. Michel, and W. Nazarewicz, Phys. Rev. **C96**, 024308 (2017).
- [17] S.M. Wang, N. Michel, W. Nazarewicz, and F.R. Xu, Phys. Rev. **C96**, 044307 (2017).
- [18] D. Hove, E. Garrido, P. Sarriguren, D.V. Fedorov, H.O. Fynbo, A.S. Jensen, and N.T. Zinner, Phys. Rev. **C93**, 034330 (2016).
- [19] A. Adahchour and P. Descouvemont, Phys. Rev. **C96**, 054319 (2017).
- [20] G.F. Bertsch and H. Esbensen, Ann. Phys. (N.Y.) **209**, 327 (1991).
- [21] K. Hagino and H. Sagawa, Phys. Rev. **C72**, 044321 (2005).
- [22] H. Sagawa and K. Hagino, Euro. Phys. J. **A51**, 102 (2015).
- [23] H. Esbensen, G.F. Bertsch, and K. Hencken, Phys. Rev. **C56**, 3054(1997).

- [24] H. Esbensen and G.F. Bertsch, Nucl. Phys. **A542**, 310 (1992).
- [25] P. Ring and P. Schuck, *The Nuclear Many-Body Problem* (Springer-Verlag, Berlin, 1980).
- [26] K. Hagino and H. Sagawa, Few-Body Systems **57**, 185 (2016).
- [27] H.T. Johansson *et al.*, Nucl. Phys. **A842**, 15 (2010); Nucl. Phys. **A847**, 66 (2010).
- [28] Z. Kohley *et al.*, Phys. Rev. Lett. **109**, 232501 (2012).
- [29] A.A. Korshennikov *et al.*, Phys. Lett. **B326**, 31 (1994).
- [30] H. Bohlen *et al.*, Prog. Part. Nucl. Phys. **42**, 17 (1999).
- [31] M.S. Golovkov *et al.*, Phys. Rev. **C76**, 021605(R) (2007).
- [32] T. Al Kalanee *et al.*, Phys. Rev. **C88**, 034301 (2013).
- [33] L. Chen *et al.*, Phys. Lett. **B505**, 21 (2001).
- [34] E. Uberseder *et al.*, Phys. Lett. **B754**, 323 (2016).
- [35] K. Hagino, N. Takahashi, and H. Sagawa, Phys. Rev. **C77**, 054317 (2008).
- [36] T. Nakamura *et al.*, Phys. Rev. Lett. **96**, 252502 (2006).
- [37] K. Hagino and H. Sagawa, Phys. Rev. **C76**, 047302 (2007).
- [38] C.A. Bertulani and M.S. Hussein, Phys. Rev. **C76**, 051602(R) (2007).
- [39] M. Pfützner, M. Karny, L.V. Grigorenko, and K. Riisager, Rev. Mod. Phys. **84**, 567 (2012).
- [40] A. Spyrou *et al.*, Phys. Rev. Lett. **108**, 102501 (2012).
- [41] Z. Kohley *et al.*, Phys. Rev. Lett. **87**, 011304(R) (2013).
- [42] Y. Kondo and T. Nakamura, private communications.